COMPUTATIONAL FLUID DYNAMICS MODELING OF BIOMASS CO-FIRING IN A 300 MW PULVERIZED COAL FURNACE

by

Jinyu SUN[a,b*], Xiaojun ZHAO[b], and Dongfa XUE[b]

[a] MOE Key Laboratory of Thermo-Fluid Science and Engineering, Xi'an Jiaotong University, Xi'an, China
[b] Nandian Synthesis Energy Utilization Co., Ltd., Guangdong, Guangzhou, China

Original scientific paper
https://doi.org/10.2298/TSCI2205179S

Biomass energy is one of the most accessible and readily available carbon-neutral energy options as a RES. It is regarded as a viable alternative fuel for coal combustion, particularly for biomass co-firing with pulverized coal, with numerous applications. The CFD can provide reasonably accurate solutions to complex thermo-chemical-fluid interactions, which is useful for understanding the design or retrofit of boilers and can save time, money, and effort. In this study, a CFD simulation of a 300 MW pulverized coal boiler with biomass co-firing was performed to investigate the impact of biomass co-firing with coal, considering the biomass co-firing ratio, mixing effect, and feeding temperature. The results show that the flow field in the furnace does not change significantly under different biomass blending ratio. Biomass co-firing can reduce peak temperatures in the furnace and make the temperature distribution more uniform. The concentration of unburned carbon in the furnace decreases as the biomass blending ratio increases. Furthermore, biomass blending has a significant impact on nitrogen oxide reduction, with NO_x emissions reduced by 20% and 28%, respectively, when the biomass blending ratio is 15% and 30%. The change of parameters inside the furnace caused by the reduction of biomass powder feeding temperature about 80 K is not significant. On the other hand, co-firing biomass with coal, reduces the risk of biomass spontaneous combustion while maintaining the furnace combustion stability and boiler combustion efficiency. The optimum ratio of biomass co-firing ration is deduced in this study is up to 20%.

Key words: *CFD, numerical simulation, biomass, coupling mixing firing, combustion characteristic*

Introduction

Coal-fired power plants emit a significant amount of CO_2, which is one of the major greenhouse gases contributing to global climate change. To keep CO_2 emissions under control, the focus of research should shift from conventional fuels (fossil fuels) to renewable and sustainable energy resources. Biomass is an easily accessible, low-cost, and readily available renewable energy resource [1]. Biomass is nearly carbon neutral because it emits the same amount of CO_2 during combustion as it absorbs through photosynthesis during its growth. Furthermore, it is produced in a sustainable manner because harvested biomass is replaced with a new generation of plants. Furthermore, biomass can accommodate a variety of agricultural or forestry

* Corresponding author, e-mail: sunjy@csg.cn

residues that would otherwise decompose and produce a large amount of methane, a greenhouse gas that is more potent than CO_2.

In China, biomass resources are nearly four times the total energy consumption, but only 5% of total biomass resources are used for energy production [2]. Furthermore, China remains a large agricultural country, and wheat stalks and agricultural waste can provide a significant amount of fuel each year. However, researchers have begun to pay attention to the environmental pollution caused by burning straw in open spaces when it is no longer useful in farmland. Direct combustion in furnaces is considered the most cost-effective method of biomass utilization due to previous experience gained from coal combustion as well as lower investment costs [3]. However, because biomass contains a higher percentage of alkali metals [4, 5] and has a lower calorific heating value, burning only biomass could result in slagging and fouling issues in heat exchangers, as well as insufficient combustion gas temperature [6]. So far, in terms of efficiency and investment cost, the co-firing approach, which refers to the partial substitution of coal by biomass, has become a widely preferred choice for burning biomass [7]. Co-firing biomass with fossil fuels in existing power plants is an appealing option for achieving the urgent near-term targets which is to increase the shares of renewable energy sources in the energy system and reducing CO_2 emissions [8].

Co-firing can be implemented in existing power plants with only minor modifications to biomass handling, milling, and injection facilities. Biomass co-firing has been carried out successfully in over 200 installations worldwide for a wide range of fuel combinations, either in pilot tests or as part of commercial operations [9]. Though issues such as biomass transportation costs and milling difficulties may arise, these can be addressed by paying close attention to the fuels, design, and operating conditions used in the burners and boilers [10]. Biomass co-firing has a number of advantages, including the ability to increase the share of renewable energy in the conventional energy portfolio, to be used more efficiently in coal-fired plants than direct biomass-fired plants, to save high capital costs by utilizing existing plant infrastructure, and to reduce CO_2, SO_2, and NO_x emissions [11]. However, co-firing has a number of drawbacks, including fuel handling and storage issues, a reduction in overall combustion efficiency, ash-related issues, pollutant emissions, and carbon burnout. As a result, special attention must be paid to the change in combustion characteristics when co-firing biomass with coal in an existing boiler.

Biomass typically has a higher volatile content and O/C ratio than coal, resulting in higher reactivity at lower ignition temperatures, arising in combustion instability [12]. Furthermore, because larger particles have a lower surface-to-volume ratio, the relative heat loss to heat generation within the particles is reduced [13]. Furthermore, due to the difficulty of grinding, the injected biomass particle size is typically larger than that of the injected coal, necessitating a longer burnout time for biomass particles [14]. Furthermore, due to the lower heating value of biomass, the biomass feeding rate in co-firing must be much higher than the replaced coal. As a result, in biomass co-firing tests, a low burnout ratio is frequently predicted [15]. To study all these uncertainties in biomass co-firing experimentally, it is very difficult, expensive, laborious and time taking. On the other hand, CFD can provide reasonably accurate solutions to complex thermo-chemical-fluid interactions, which is useful for understanding boiler design or retrofit.

The CFD is a cost-effective tool for gaining a better understanding of co-firing combustion issues and problems [16]. Various simulation studies of pulverized coal combustion in full scale tangential fired furnaces, for example [17-19], have been conducted. However, little work has been done on straw-coal co-firing, with few papers based on small test furnaces are published. Backreedy *et al.* [20] investigated the discrepancy between the errors generated in the simulation of biomass particle size and the actual experiment. On the basis of air fuel combustion and oxygen-enriched combustion, Johansson *et al.* [21] improved the weighted grey gas model (WSGGM) for the all-oxygen fuel combustion model. Ghenaic and Janajrehr [22] used a furnace to simulate the mixing and combustion of pulverized coal and biomass particles. The static mixer can achieve efficient mixing in the furnace because the mixing occurs in turbulent flow, resulting in more efficient mixing. Although biomass can be considered analogous to coal for the combustion process, however, the size and shape of the biomass are expected to influence the combustion dynamics and emissions [23].

In this study, a CFD simulation of a 300 MW pulverized coal boiler with biomass co-firing was performed to investigate the impact of biomass co-firing with coal, considering the biomass co-firing ratio, mixing effect, and feeding temperature. The research presented in this paper will be useful in further optimizing the utilization of biomass in local full-scale pulverized coal furnaces.

Model and setting

In this section, properties of coal *i.e.*, proximate and ultimate analysis, the composition of coal ash and additives, ash preparation and characterization method are illustrated.

Furnace structural parameters and fuel characteristics

The simulation study was carried out for a 300 MW Tangentially fired boiler. Figure 1 illustrated the general geometry of the furnace. Because the research is limited to the burning part of the furnace, the geometry considered is up to the flue gas rising part of the furnace. The width and length of the burner area are approximately 13.5 m and 14 m, respectively, with the total height of the furnace being approximately 55 m.

The pulverized coal furnace is fitted with staged over fire air (SOFA) nozzle, and the primary air and secondary air nozzles are cross-arranged, as shown in fig 1. There are two sets of burners from bottom to top, and each set of burners includes two primary air nozzles and three secondary air nozzles arranged crosswise. Figure 1(b) shows the partial configuration of the burners, where port of the primary air is marked with a single letter, while secondary air is marked with two letters, and SOFA is marked separately. The nozzles from bottom to top are AA, A, AB, B, BC, C, CC, DC, E, EE, F, FE, G, GG, SOFA1, SOFA2, SOFA3. Ports B and C are designated for biomass feeding, and the biomass co-firing ratio is adjusted in accordance with the amount of biomass fed through the aforementioned burners.

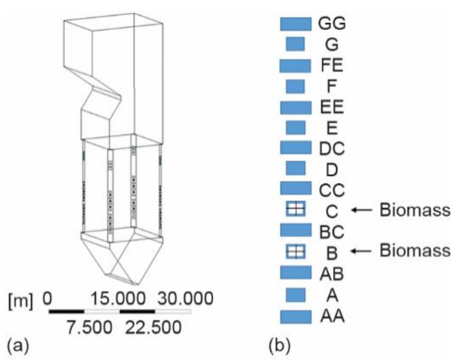

Figure 1. (a) Geometric structure of the furnace and (b) structure configuration of the lower burner group

Yulin coal which is abundant in the central and western regions of china is used in this paper. However, due to the lack of relevant production data of biomass for power generation in China, local data are not easy to obtain, so the olive residue, which is similar to straw composition and combustion characteristics, is used as the blended biomass, and the combustion characteristics of the latter have been quite fully studied. Fuel analysis of pulverized coal and biomass is shown in tab. 1, and particle size parameters are shown in tab. 2.

Table 1 Proximate analysis and ultimate analysis

Fuel	Ultimate analysis [%]					Proximate analysis [%]			
	C_{daf}	H_{daf}	O_{daf}	N_{daf}	S_{daf}	V_{ar}	FC_{ar}	A_{ar}	M_{ar}
Coal	79.6	6.7	11.9	1.0	0.8	35.2	52.0	4.5	8.3
Biomass	54.3	6.63	36.9	1.95	0.22	65.4	18.7	6.9	9.0

V – volatile, FC – fixed carbon, A – ash, M – moistures, ar – as received base.

Table 2. Fuel particle size parameters

Fuel	Particle size parameters			
	d_m [μm]	d_{max} [μm]	d_{min} [μm]	Distribution index
Coal	42	300	10	1.36
Biomass	100	150	75	2.3

Geometry and meshing

Establishment of geometric model

Because there are numerous structures inside the boiler, the water-cooled wall of the furnace is not completely smooth. However, due to the smaller effect, this paper neglects it and considers the wall to be a flat plane. The actual burner is often equipped with a number of auxiliary equipment for the primary air nozzle in order to improve the fuel ignition stability and ensure that the jet does not twist easily. Common methods include increasing the blunt body, using a cyclone burner, and so on. It is very difficult to consider every minute geometric specification of the real burner in generating the geometry for simulation. Therefore, for simplification it is decided to consider the burner geometry as a rectangular nozzle, which can meet the precision requirement.

Meshing

In this model, a structured grid is used to divide the grid. The furnace is divided into three areas for block division, namely, the cold ash hopper to the burner area, the burner area and the upper part of the burner area. The division of the burner area is more complicated: firstly, the cross-section of the furnace should be divided, and then the upper and lower boundaries of each burner should be cut to keep the grid parallel in the direction of the vertical axis. For the division of the cross-section, after considering the flow field distribution of the imaginary circle of the tangential furnace with four corners, the partitioning was planned and the area with intense combustion and large mass-flow was encrypted. The division results were shown in fig. 2(a). After inspection, the grid quality reached a high level without negative volume. The inspection results, as shown in fig. 2(b), were above 0.6, which met the requirements of high quality.

Model setting and simulation

After solid fuel (such as pulverized coal) has been injected into the furnace, a series of interconnected processes occurred, including dynamic interaction between gas and particles, turbulence, heat transfer, and pollutant formation. During the numerical simulation process, the model should consider all of these processes that occur during combustion.

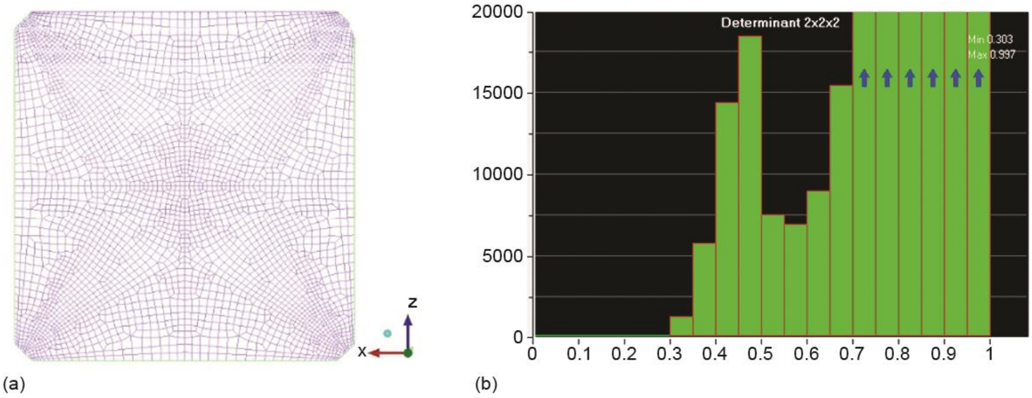

Figure 2. (a) Grid division of the *Z*-axis profile near the burner in the furnace and (b) grid quality inspection results in the furnace

Governing equation

The governing equations involved in the current simulation include mass, momentum, and energy conservation equation. The turbulent model is used for the combustion process inside the furnace because the mixing of fuel and gases is very high and the Reynolds number is higher than the laminar and transition flow. The most commonly used governing equation to describe turbulence is the standard *k*-model. The equation is expressed in eqs. (1) and (2), respectively:

$$\frac{\partial(\rho k)}{\partial t}+\frac{\partial(\rho k u_i)}{\partial x}=\frac{\partial}{\partial x}\left[\left(u+\frac{u_i}{\sigma_z}\right)\frac{\partial k}{\partial x_j}\right]+G_\mathrm{k}+G_D-\rho\varepsilon-Y_M+S_k \tag{1}$$

$$\frac{\partial(\rho \varepsilon)}{\partial t}+\frac{\partial(\rho \varepsilon u_i)}{\partial x}=\frac{\partial}{\partial x}\left[\left(u+\frac{u_i}{\sigma_\varepsilon}\right)\frac{\partial z}{\partial x_j}\right]+C_{1z}\frac{\varepsilon}{k}(G_\mathrm{k}+C_3G_\mathrm{b})-C_{2z}\rho\frac{\varepsilon^2}{k}+S_z \tag{2}$$

where ρ is the density of fluid, k – the turbulent kinetic energy, G_k – the generation of turbulence kinetic energy, G_b – the generation of turbulence kinetic energy due to buoyancy, ε – the dissipation rate, σ_z and σ_ε – the turbulent Prandtl numbers for k and ε, μ_i – the turbulent viscosity coefficient, and C_x – the empirical coefficient, among them C_{1z} = 1.44, C_{2z} = 1.92, C_μ = 0.09.

Discrete phase model

In this paper, Euler's method is used to solve the continuous phase transport equation, but the fuel particles are tracked by Lagrange's method. Biomass pellets are not usually spherical, but are generally considered to be filamentous. Therefore, biomass pellets used for co-combustion are often considered to be much larger and more irregular in shape than pulverized coal pellets. Yin *et al.* [24] established a model to track non-spherical particles in fluid-flow and found that for biomass particles with a diameter of several hundred microns, the heat and mass transfer within the particles did not have a critical effect on the simulation results in the case of combustion. In the environment discussed in this paper, biomass particles are small in size and almost spherical in shape. In all working conditions, the Binger number is far lower than 0.1, which can be considered that the particle conforms to the isothermal hypothesis, so the influence of heat and mass transfer inside the particle on the simulation accuracy is not considered [25]. Since biomass particles are assumed to be spherical, only gravity and standard viscous force are retained in the motion equation of biomass particles [8], which is the same as the tracking method of pulverized coal particles in this study.

Devolatilization model

Material component transport provided by FLUENT is used to model solid fuel devolatilization. Material component transport regards volatile as a substance with a single chemical formula, namely CH_xO_y, where x and y can be any positive real numbers [26]. For a given type of coal, it can give the formula for any organic matter consisting of C, H_2, and O_2. In a simulated reaction for one-step transport of material components, the conceptually existing material would undergo a one-step reaction with O to produce CO_2 and water.

Heat transfer model

The WSGGM [10] model is used to model the gas radiation and DO model is used to model the heat transfer through radiation.

The NO reaction model

Because of the magnitude difference between the NO_x formation reaction and the previously described model, its numerical simulation process can be post-processing calculation under the flow field, temperature field, and component field of the model iterative convergence.

Simulation of operating conditions and boundary conditions

The dimensions and burner configuration of the furnace, in which pulverized coal and biomass are fed through a primary slot, have already been depicted in fig. 1. According to the design parameters of the boiler and the relevant air supply criteria, the theoretical combustion air volume to the fuel is 1:1.15. It is fed through primary and the secondary air nozzle, respectively. The biomass powder feeding adopts a split feeding method, such that, it is fed from the B-layer burner or the C-layer burner. Different working conditions and corresponding parameters are given in tabs. 3 and 4. Under different working conditions, it is ensured that the total energy fed into the furnace through the fuel remains unchanged, and the co-

Table 3. Conditions parameters used in numerical simulation

Boundary conditions	Fuel	B-layer burner		C-layer burner		Convert biomass co-firing ratio
		Mass-flow [th^{-1}]	Powder feeding temperature [K]	Mass-flow [th^{-1}]	Powder feeding temperature [K]	
1	Coal	3.8	378	3.8	378	0
2	Biomass	5.9	378	3.8	378	15%
3	Biomass	5.9	378	5.9	378	30%
4	Biomass	5.9	293	3.8	378	15%

firing ratio is changed by feeding the powdered coal/biomass through the B-layer and the C-layer. The specific boundary condition settings of the two layers (B and C) are shown in tab 3. Except for the nozzles of the B- and C-layers, the boundary conditions for other feeding nozzles are same as shown in tab. 4, under all working conditions.

Table 4. Furnace boundary conditions

Port	Air speed [ms^{-1}]	Inlet air temperature [K]	Mass-flow [th^{-1}]
Primary air			
A	21	378	4.1
B	24	See tab. 5	See tab. 5
C	24	See tab. 5	See tab. 5
D	24	378	3.8
E	24	378	3.8
F	24	378	3.8
G	24	378	3.8
Secondary air			
AA	45	573	0
AB	45	573	0
BC	45	573	0
CC	45	573	0
DC	45	573	0
EE	45	573	0
FE	45	573	0
GG	45	573	0
SOFA	45	578	0

Simulation results and discussion

In order to explore the mentioned problems, this section carried out the simulation of the biomass co-fired with coal, the powder feeding temperature under different working conditions, the flow field, temperature field, concentration of various material components, tracked particles, unburned carbon, fuel burnout, and NO_x emission.

Influence of biomass mixing burning ratio

This section mainly explores the effects of different biomass mixing and firing ratios on flow characteristics, temperature field, material component distribution, char concentration, fuel burnout and NO_x emissions. The working conditions corresponding to the analysis are 100% coal, 15% and 30% biomass co-firing ratio, and feeding temperature.

Dynamic flow characteristics

Figure 3 shows the difference of velocity scalar cloud images in the XZ plane by feeding the 100% coal and 15% biomass co-firing. By comparing fig. 3(a) with fig. 3(b), it is noticed that the flow field distribution near the burner are nearly same for both the figures while

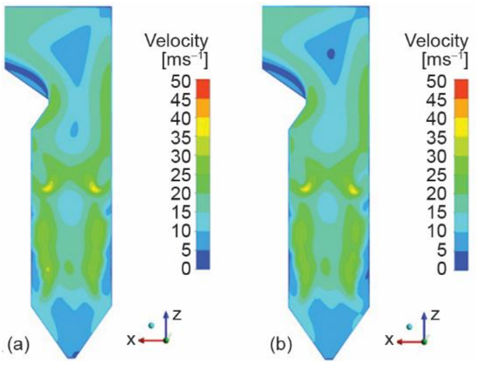

Figure 3. Velocity distribution under by feeding (a) 100 % coal and (b) 85% coal 15% biomas

the area near the ash hopper and upper part of the furnace it is prominently different. The volumetric flow rate of flue gas is 1635 kg/s and 1600 kg/s by feeding the 100% coal and 85% coal with mixing 15% biomass, respectively. It portrays that biomass co-firing alter the composition of flue gas that resulting the variation in the flow field at the upper and lower part of the furnace.

Temperature field

Figure 4 depicts the temperature field distribution in the furnace under various operating conditions. The temperature field distribution confirms the study expectations. Overall, the flame is stable, and the flame filling degree in the furnace is satisfactory. The temperature of the furnace near the burner is higher, which can be attributed to the intense combustion of pulverized coal and biomass, as well as their volatiles. In general, the temperature in the furnace rises and then falls from the bottom to the top of the furnace. This is because the fuel must absorb heat from the bottom to the top of the furnace to preheat and devolatilize before catching fire. Heat is released at this time. When the results of different working conditions are compared, it is induced that as the proportion of biomass mixed firing increases, the temperature in the furnace decreases continuously, and the temperature of the flue gas at the outlet also decreases. As the biomass mixing ratio increases, the peak temperature in the furnace decreases continuously, and the temperature distribution becomes more uniform.

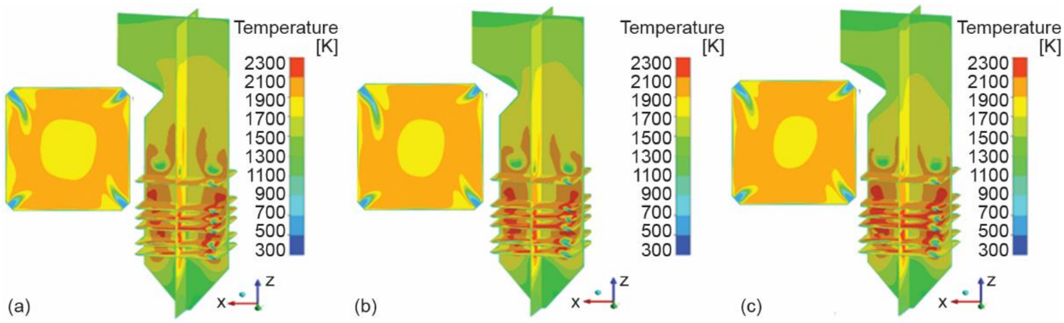

Figure 4. Temperature distribution in furnace and at the cross-section near the height of SOFA burner under different working conditions; (a) coal, (b), 15% biomass, and (c) 30% biomass

Further, the temperature contours of the cross section near the SOFA nozzle is located and illustrated in larger detail that how the temperature field changes with the proportion of biomass mixed and burned. The area of the central low temperature tangential circle decreases as the biomass mixing ratio increases, and the central temperature of the planar furnace is 1753 K, 1782 K, and 1798 K under different working conditions. The temperature distribution in the planar furnace is more uniform, and the flame fullness is greater. The proportion of volatiles combustion in the heat release increases as the proportion of biomass mixing combustion increases, while the proportion of char combustion decreases. The volume of volatiles combustion in the furnace has increased, and the temperature distribution in the furnace has become more uniform, resulting in a reduction in the area of the central low temperature area.

Carbon concentration distribution

As can be seen from fig. 5, the char in the furnace is mainly distributed in the central area of the furnace and the ash hopper area, among which the concentration near the burner nozzle is obviously higher, followed by the ash hopper, and the char concentration in the upper part of the furnace is almost 0.

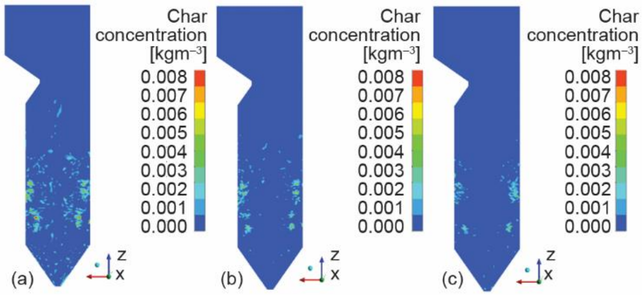

Figure 5. Carbon concentration distribution in the furnace under different working conditions; (a) coal, (b), 15% biomass, and (c) 30% biomass

It can be considered that after the fuel is ejected from the nozzle of the primary air burner in the furnace, it first carries out convection and radiation heat transfer with the material and structure inside the furnace to obtain heat and then carry out the process of devolatilization. This process is more intense near the nozzle of the burner, resulting in a high char concentration there. As the generated char burns, some particles with small particle size burn more completely. As the flow field in the furnace flows to the furnace outlet, the upper part of the furnace is almost completely burnt out, with a low char concentration. Some particles with larger particle sizes, on the other hand, may not burn completely, and the air-flow is insufficient to provide enough force to contend with the gravity it is affected by, so they fall into the cold ash bucket area. Some particles that cannot be burned out fall into the cold ash bucket area, forming a medium concentration zone. By comparing the distribution of char concentration in the furnace under different working conditions, it is found that as the biomass mixing ratio increases, the overall char concentration in the furnace decreases significantly, and the area with higher char distribution in the furnace gradually shrinks. The overall volatile content of the fuel increases as the biomass mixing and firing proportion increases, and the ignition position of the fuel advances and moves towards the nozzle. One of the results brought by high volatiles is that the temperature distribution in the furnace is more uniform, and the char combustion is also more intense, which can make it burn out in a faster time. Since due to the low heating value of biomass and high moisture content the peak temperature area drop quickly leading to a uniform temperature profile [27]. As reflected in the cloud image, the char concentration near the burner is lower, and the char concentration distribution shows a shrinkage trend.

Influence of feeding temperature

This section investigated the effect of temperature changes on material component distribution, char concentration, and fuel combustion, as well as the impact of NO_x emissions. Because the overall distribution of parameters in the furnace was thoroughly discussed in the previous section, this section will concentrate on the differences in parameter distribution caused by different working conditions.

Temperature field

By comparing the temperature distribution cloud diagram of working Condition 2 (powder feeding temperature at B-layer is 378 K, 15% biomass) and working Condition 4 (powder feeding temperature of B-layer is 293 K, 15% biomass) in fig. 6, it can be seen that only the change of powder feeding temperature can greatly affect the temperature distribution in the furnace, and its influence range is mainly concentrated near the nozzle.

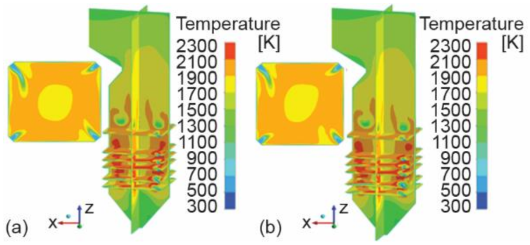

Figure 6. Temperature distribution in furnace and at the cross-section near the height of SOFA burner under different working conditions; (a) powder feeding temperature at B-layer is 378 K (15% biomass) and (b) powder feeding temperature of B-layer is 293K (15% biomass)

At the nozzle of B-layer (the second-layer at the bottom of the figure is the primary air nozzle of fuel biomass), a relatively prominent low temperature area can be seen beside the jet in working Condition 4, which is lower than that in working Condition 2, because the powder feeding temperature is lower than the temperature of the nozzle in working Condition 2, which is 80 K. The temperature field at the bottom, where the combustion has not yet been intense, may be more disturbed by such a large difference in feeding temperature. A small range of temperature difference can still be seen at the C-layer of the upper burner due to the continuous development of combustion in the furnace from the lower to the upper layer and the injection of new fuel to enhance the combustion effect, but its influence has been very limited. By comparing the two subfigures (cross-sections) in figs. 6(a) and 6(b), near the SOFA nozzle, the difference of temperature field in the two working conditions is almost invisible. Although the influence of a single one-layer nozzle's air temperature reduction of 80 K is very obvious in the local area, it can be considered as insignificant for the total temperature in the furnace.

Component concentration

The O_2 concentration profile

By comparing the two subfigures in fig. 7, it can be clearly found that the O_2 concentration distribution of the two Conditions 2 (powder feeding temperature at B-layer is 378 K, 15% biomass) and working Condition 4 (powder feeding temperature of B-layer is 293 K, 15% biomass) are almost same, but the oxygen concentration in working Condition 4 has higher at the outlet. The difference between working Conditions 2 and 4 is that the temperature of biomass powder feeding in B-layer is different. The powder feeding temperature in working Condition 4 is lower, this might be possible that the combustion of fuel starts later as compared to the Condition 2, therefore the outlet oxygen concentration is higher in working Condition 4 compared to 2.

The CO concentration distribution

Comparing the two subgraphs in fig. 8, the numerical simulation results show that the CO concentration distribution under the two working conditions are almost same. However, the CO concentration under working Condition 2 (powder feeding temperature at B-layer is 378 K, 15% biomass) is slightly higher than that under the working Condition 4 (powder feeding

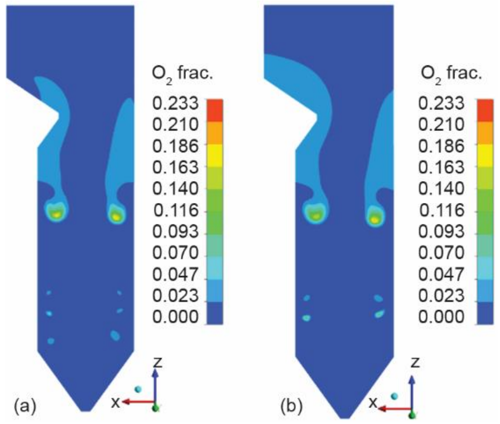

Figure 7. The O_2 concentration distribution in the furnace under different working conditions; (a) powder feeding temperature at B-layer is 378 K (15% biomass) and (b) powder feeding temperature of B-layer is 293 K (15% biomass)

temperature of B-layer is 293 K, 15% biomass) in a small area near the burner. Combined with the analysis of the two working conditions, it can be considered that this slight difference is due to the slight decrease of the temperature in the furnace near the nozzle and the temperature of local combustion due to the powder feeding at a lower temperature, which is not conducive to the generation of CO in dynamics and reduces the concentration of CO near the burner. Since the concentration of CO at the outlet is very low, the influence of cold air powder feeding on combustion stability can be ignored.

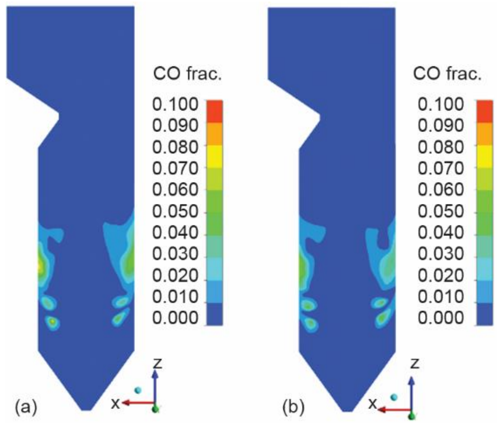

Figure 8. The CO concentration distribution in the furnace under different working conditions; (a) powder feeding temperature at B-layer is 378 K (15% biomass) and (b) powder feeding temperature of B-layer is 293 K (15% biomass)

The C concentration distribution and burnout situation

By comparing the two sub-figures in fig. 9, it can be found that with the change of biomass feeding temperature, the distribution of char concentration in the furnace does not change significantly. By comparing the distribution of char concentration near the nozzle of burner in B-layer, it can be found that the peak of char concentration can be slightly delayed by cold air powder feeding as shown in fig. 9(b). The decrease of the powder feeding temperature makes a local low temperature zone appear near the burner, which will slightly delay the devolatilization process of the fuel, and then delay the rise process of the char concentration along with the fuel jet injection. Generally speaking, the occurrence of this situation is closely related to the difference of temperature field, and has little influence on the distribution of char concentration in furnace.

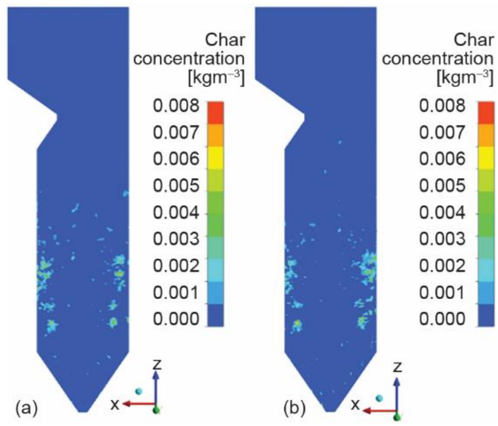

Figure 9. The C concentration distribution in the furnace under different working conditions; (a) powder feeding temperature at B-layer is 378 K (15% biomass) and (b) powder feeding temperature of B-layer is 293 K (15% biomass)

Conclusions

In this study, a CFD simulation of a 300 MW four-corner tangential pulverized coal boiler with biomass co-firing was performed to investigate the impact of biomass co-firing with coal, considering the biomass co-firing ratio (0%, 15%, and 30%), mixing effect, and feeding temperature. The conclusions are as follows.

- The flow field in the furnace does not change significantly under different biomass mixing ratio. The biomass co-firing can significantly reduce the peak temperature in the furnace and make the temperature distribution profile more uniform.
- The char concentration decreased with the increase of biomass co-firing ratio. Further, the biomass co-firing has a significant effect on the reduction of NO_x emissions, and the biomass mixing combustion ratio at 15% and 30% can reduce NO_x emissions by 20% and 28%, respectively.
- The changes in parameters inside the furnace no noticeable impact by lowering the biomass feeding temperature by about 80 K. Co-firing biomass with coal can effectively reduce the risk of biomass spontaneous ignition while having little impact on the furnace's combustion stability or the boiler's combustion efficiency.
- The optimum biomass co-firing ratio is up to 20%, because more than that causes corrosion, milling, collection, and transportation issues.

References

[1] Bhuiyan, A. A., Naser, J., CFD Modelling of Co-Firing of Biomass with Coal under Oxy-Fuel Combustion in a Large Scale Power plant, *Fuel, 159* (2015), Nov., pp. 150-168
[2] Xingang, Z., *et al.*, Focus on Situation and Policies for Biomass Power Generation in China, *Renewable and Sustainable Energy Reviews 16* (2012), 6, pp. 3722-3729
[3] Black, S., *et al.*, Effects of Firing Coal and Biomass under Oxy-Fuel Conditions in a Power Plant Boiler Using CFD Modelling, *Fuel 113* (2013), Nov., pp. 780-786
[4] Zi, J., *et al.*, Slagging Behavior and Mechanism of High-Sodium-Chlorine Coal Combustion in a Full-Scale Circulating Fluidized Bed Boiler, *Journal of the Energy Institute, 93* (2020), 6, pp. 2264-2270
[5] Zhang, J., *et al.*, Hot Corrosion Behaviors of TP347H and HR3C Stainless Steel with KCl Deposit in Oxy-Biomass Combustion, *Journal of Environmental Management, 263* (2020), June, ID 110411
[6] Zi, J., *et al.*, Effects of Temperature and Additives on Ash Transformation and Melting of High-Alkali-Chlorine Coal, *Thermal Science, 24* (2020), 6A, pp. 3501-3510
[7] Bhuiyan, A. A., Naser, J., Computational Modelling of Co-Firing of Biomass with Coal under Oxy-Fuel Condition in a Small Scale Furnace, *Fuel, 143* (2015), Mar., pp. 455-466

[8] Zheng, S., *et al.*, Experimental Investigation of the NO_x Formation and Control during the Self-Sustaining Incineration Process of N-Containing VOCs (dimethylformamide), *Fuel, 315* (2022), May, ID 123149
[9] ***, IEA Bioenergy Task 32: Biomass Combustion and Co-Firing, Database of Biomass Co-Firing, http://www.ieabcc.nl/ (last visit May 2022)
[10] Alvarez, L., *et al.*, Biomass Co-Firing under Oxy-Fuel Conditions: A Computational Fluid Dynamics Modelling Study and Experimental Validation, *Fuel Processing Technology*, *120* (2014), Apr., pp. 22-33
[11] Wang, X., *et al.*, Experimental Study and Design of Biomass Co-Firing in a Full-Scale Coal-Fired Furnace with Storage Pulverizing System, A*gronomy, 11* (2021), 4, ID 810
[12] Li, J., *et al.*, Studies of Ignition Behaviour of Biomass Particles in a Down-Fire Reactor for Improving Co-Firing Performance, *Energy & Fuels, 30* (2016), 7, pp. 5870-5877
[13] Momeni, M., *et al.*, Experimental Study on Effects of Particle Shape and Operating Conditions on Combustion Characteristics of Single Biomass Particles, *Energy & Fuels, 27* (2013), 1, pp. 507-514
[14] Magalhaes, D., *et al.*, Comparison of Single Particle Combustion Behaviours of Raw and Torrefied Biomass with Turkish Lignites, *Fuel, 241* (2019), Apr., pp. 1085-1094
[15] Tu, Y., *et al.*, Effect of Biomass Co-Firing Position on Combustion and NO_x Emission in a 300 MWe Coal-Fired Tangential Boiler, *Asia-Pacific Journal of Chemical Engineering, 17* (2021), 1, ID e2743
[16] Tabet, F., Gokalp, I., Review on CFD Based Models for Co-Firing Coal and Biomass, *Renewable and Sustainable Energy Reviews, 51* (2015), Nov., pp. 1101-1114
[17] Asotani, T., *et al.*, Prediction of Ignition Behavior in a Tangentially Fired Pulverized Coal Boiler Using CFD, *Fuel*, *87* (2008), 4, pp. 482-490
[18] Zhou, H., *et al.*, Numerical Simulation of the NO_x Emissions in a 1000 MW Tangentially Fired Pulverized-Coal Boiler: Influence of the Multi-Group Arrangement of the Separated over Fire Air, *Energy & Fuels, 25* (2011), 5, pp. 2004-2012
[19] Belosevic, S., *et al.*, Three-Dimensional Modeling of Utility Boiler Pulverized Coal Tangentially Fired Furnace, *International Journal of Heat and Mass Transfer, 49* (2006), 19, pp. 3371-3378
[20] Backreedy, R. I., *et al.*, Co-Firing Pulverized Coal and Biomass: A Modeling Approach, *Proceedings, of the Combustion Institute, 30* (2005), 2, pp. 2955-2964
[21] Johansson, R., *et al.*, Account for Variations in the H_2O to CO_2 Molar Ratio when Modelling Gaseous Radiative Heat Transfer with the Weighted-Sum-Of-Grey-Gases Model, *Combustion and Flame, 158* (2011), 5, pp. 893-901
[22] Ghenai, C., Janajreh, I., CFD Analysis of the Effects of Co-Firing Biomass with Coal, *Energy Conversion and Management, 51* (2010), 8, pp. 1694-1701
[23] Gubba, S. R., *et al.*, Numerical Modelling of the Co-Firing of Pulverized Coal and Straw in a 300 MWe Tangentially Fired Boiler, *Fuel Processing Technology, 104* (2012), Dec., pp. 181-188
[24] Yin, C., *et al.*, Use of Numerical Modeling in Design for Co-Firing Biomass in Wall-Fired Burners, *Chemical Engineering Science, 59* (2004), 16, pp. 3281-3292
[25] Gera, D., *et al.*, Effect of Large Aspect Ratio of Biomass Particles on Carbon Burnout in a Utility Boiler, *Energy & Fuels, 16,* (2002), 6, pp. 1523-1532
[26] Ma, L., *et al.*, Modelling Methods for Co-Fired Pulverized Fuel Furnaces, *Fuel, 88* (2009), 12, pp. 2448-2454
[27] Wang, X., *et al.*, Numerical Study of Biomass Co-Firing Under Oxy-MILD Mode, *Renewable Energy, 146* (2020), Feb., pp. 2566-2576

Paper submitted: February 17, 2022
Paper revised: May 25, 2022
Paper accepted: June 5, 2022